Progress In Electromagnetics Research Letters, Vol. 94, 125–131, 2020

High Sideband Suppression Dual-Mode Filters Using New CPW Resonator

Yuanbao Chen, Shuang Huang, Gang Xie, and Jia Chen*

Abstract—A novel class of dual-mode filters with improved high frequency sideband suppression response making use of a coplanar waveguide (CPW) square loop resonator is presented. The resonator is placed on the bottom plane and inside the defected area of the ground. The resonant property of the CPW square loop resonator as well as the coupling property between two degenerate modes with different patch perturbation is studied in the paper. Two T-shaped orthogonal feed lines are arranged on the top plane, which not only provide proper excitation to the resonator, but also introduce an additional source-load coupling, so the proposed filter is found to have two transmission zeros at high frequency sideband and takes on an asymmetric frequency response. Such a compact dual-mode CPW square loop resonator filter operating at 2.68 GHz is designed and fabricated.

1. INTRODUCTION

In recent years, microstrip filters with dual-mode property have been widely used in the design of planar microwave filters. A dual-mode microstrip filter may be easily designed by using two degenerate modes of a single-mode microstrip resonator such as circular disk or ring, triangle, rectangular, square patches or loops. Dual-mode filter was firstly proposed using a dual-mode ring resonator by Wolff [1]. The dual-mode property has been particularly investigated and developed for single [2, 3] or dual-band [4, 5] bandpass filters to obtain high frequency selectivity near passbands by using one or more transmission zeros on the low or high side of passbands. In [6], a cross-slotted patch resonator is successfully developed to demonstrate the simultaneous size and loss reduction, and further to build a novel dual-mode bandpass patch filter by suitably selecting the unequal cross-slot lengths along the two orthogonally diagonal planes. A dual-mode dual-band bandpass filter using ridge gap structure is presented in [7], which needs only a single input and output. Many other types of single band [8–11] or dual-band [12] dual-mode filters have been studied in recent years.

However, most of the dual-mode filters have symmetrical frequency responses with a pair of transmission zeros at both bandsides or without transmission zeros. With the increased requirement of high suppression at one side of passband especially on high frequency sideband, the previous dual-mode filters need to be improved. In this paper, a novel dual-mode bandpass filter composed of a CPW square loop resonator and T-shaped feed lines is presented, which introduces a source-load coupling and has two transmission zeros on the high side of the passband. Based on the analysis of resonant and coupling properties of CPW square loop resonator, such a dual-mode filter is designed and fabricated.

2. RESONANT PROPERTY OF CPW SLR

Figure 1 shows the configuration of both the conventional microstrip square ring resonator (MS SLR) and the proposed coplanar waveguide square ring resonator (CPW SLR). The square loop resonator

Received 22 April 2020, Accepted 23 September 2020, Scheduled 10 November 2020
* Corresponding author: Jia Chen (26029432@qq.com).
The authors are with the Wuhan Second Ship Design and Research Institute, Wuhan, Hubei, P. R. China.

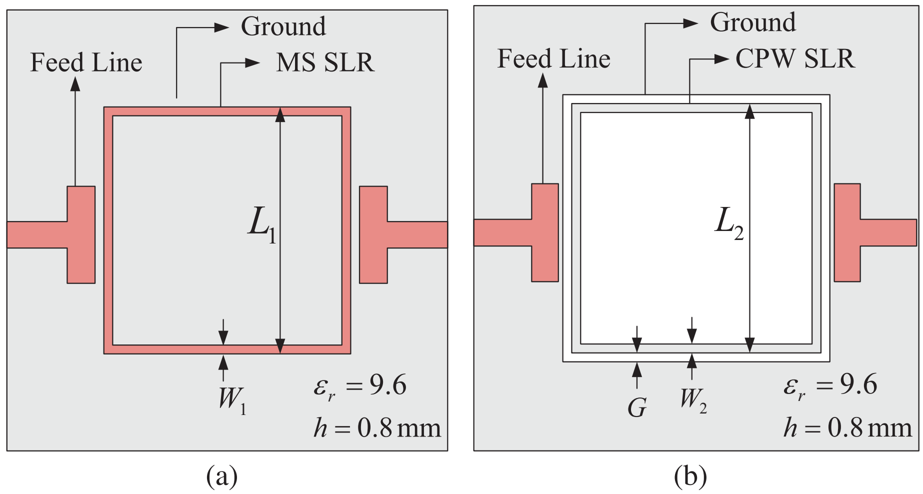

Figure 1. (a) Conventional microstrip square ring resonator. (b) Proposed coplanar waveguide square ring resonator.

consists of four identical arms with a length of L_i ($i = 1, 2$), which is located on the top plane (MS type) or inside the defected ground (CPW type). The resonator in the latter is placed at the bottom plane and coplanar with the surrounded ground. The substrate has a relative dielectric constant of 9.6 and a thickness of 0.8 mm. Different frequency responses can be obtained with various lengths of L_2, and the fundamental resonance occurs when $L_i \approx \lambda_g/4 + W_i$, where λ_g is the guided wavelength, and the resonant frequency is given by

$$f_i = \frac{c}{\lambda_g\sqrt{\varepsilon_{eff}^i}} = \frac{c}{4(L_i - W_i)\sqrt{\varepsilon_{eff}^i}} \tag{1}$$

where c is the velocity of light in free space, and ε_{eff}^i is the effective dielectric constant of the substrate. For microstrip condition, if $W_1 = 0.5$ mm, we can obtain $\varepsilon_{eff}^1 \approx 6.42$ and $f_1 = 29.597/(L_1 - 0.5)$, while for CPW condition, if $W_2 = G = 0.5$ mm, then $\varepsilon_{eff}^2 \approx 4.56$, and $f_2 = 35.11/(L_2 - 0.5)$.

The resonant properties of microstrip SLR and coplanar waveguide SLR are analyzed with the full-wave EM simulation Ansoft HFSS software and compared with each other, as compared in Fig. 2. When the sidelength L_i increases, both of the resonant frequencies decline gradually and agree with the previous calculated formula (1). This indicates that the resonant frequency of CPW SLR can be

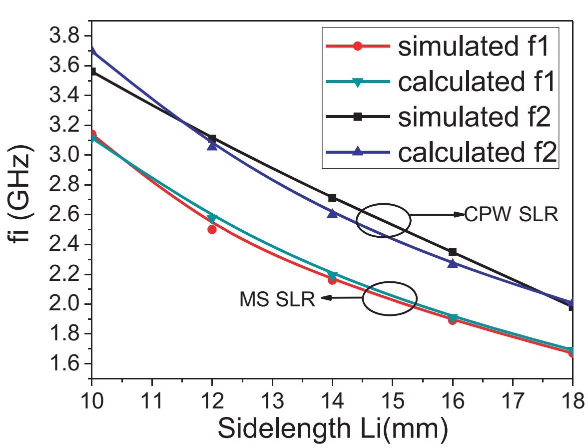

Figure 2. Comparison of resonant frequencies between MS SLR and CPW SLR.

estimated by the conventional CPW calculation methods, and it has a higher resonant frequency than MS SLR with the same sidelength.

3. COUPLING PROPERTY OF CPW SLR

As shown in Fig. 3, the current distribution pattern on the surface of two types of CPW square loop resonator filters is plotted. In this case, two feed lines are arranged orthogonally to excite two degenerate modes. Filter I introduces a patch in the corner as a perturbation while filter II introduces a cut, which leads to a split of two degenerate modes. Before mode split, the resonator at resonant frequency f_0 has the maximum current density in the middle side vertical to the symmetrically arranged ports. After mode split, the maximum current vectors at frequency f_1 of mode 1 and f_2 of mode 2 move to a pair of corners at leading diagonal or auxiliary diagonal, respectively.

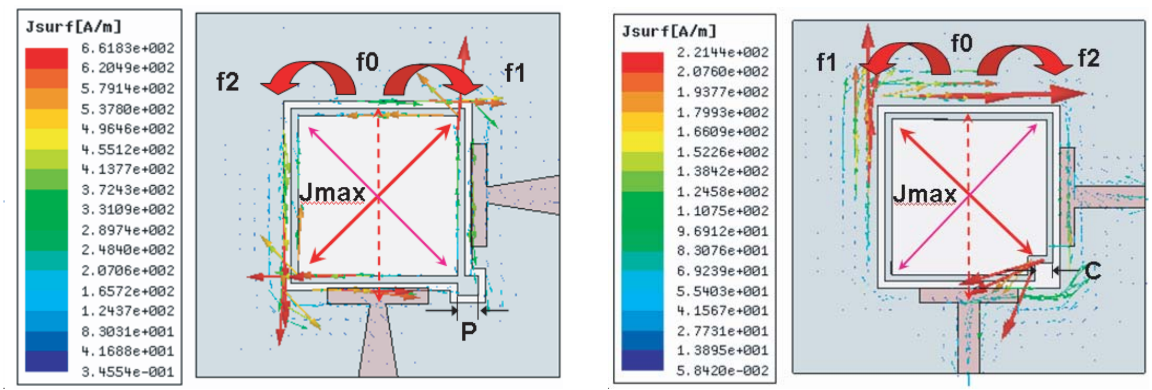

Figure 3. Current pattern of two types of dual-mode CPW SLR filters. (a) Filter I with a patch at 2.86 G. (b) Filter II with a cut at 3.0 G.

The perturbation dimension has direct influence on the frequency split as well as the coupling strength of two degenerate modes, as shown in Fig. 4. In filter I, as patch size is enlarged, the two mode frequencies split much wider, which means that the coupling coefficient increases at the same time. In filter II, with the cut size increased, the difference between two mode frequencies is wider, and the coupling coefficient goes up gradually.

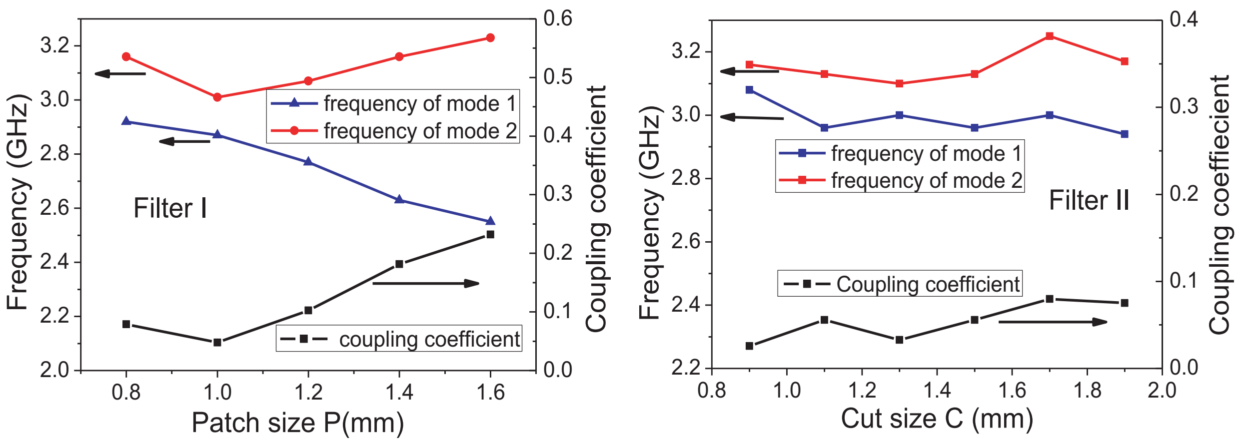

Figure 4. Coupling property of dual-mode CPW SLR filters.

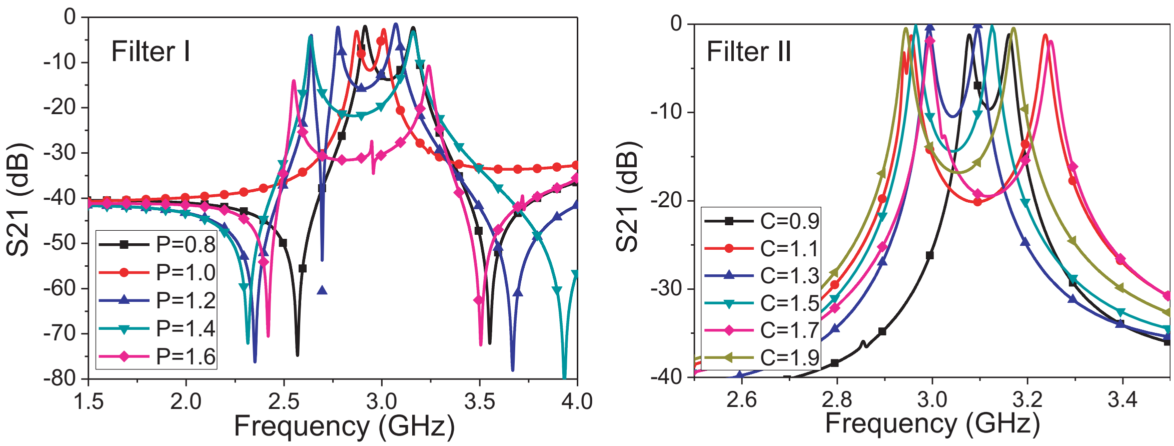

Figure 5. Coupling property of dual-mode CPW SLR filters.

In order to analyze the coupling characteristic of the CPW square loop resonator, a pair of T-shaped feed lines is arranged orthogonally on the top of the substrate and has a proper gap with respect to the square ring, which is used to provide weak external coupling to the resonator. The simulated results are shown in Fig. 5. It is seen that two resonant peaks appear in the transmission curves, which are corresponding to mode 1 and mode 2, and they shift apart as the patch or cut size increases. Moreover, a patch in filter I introduces capacitive perturbation, and two additional transmission zeros located on either side of the passband are generated. While a cut in filter II introduces inductive perturbation, there are no transmission zeros on both sides. Since filter I exhibits an elliptic characteristic, it is more suitable for high selective filter design.

4. SOURCE-LOAD COUPLING WITH T-TYPE FEED LINE

Although filter I has the advantage of high suppression on both sides of the passband, the stopband width and side sharpness are not very satisfactory. In order to realize a large enough external coupling, the T-shaped feed line must be inserted in the resonator area and has an overlapped area with the loop side, as depicted in Fig. 6. Unlike conventional dual-mode microstrip filters, the feed lines of CPW SLR filter are located on the opposite plane relative to the resonator on the bottom plane, which allows a much closer distance of the two feed lines. By this method, a source-load coupling is introduced

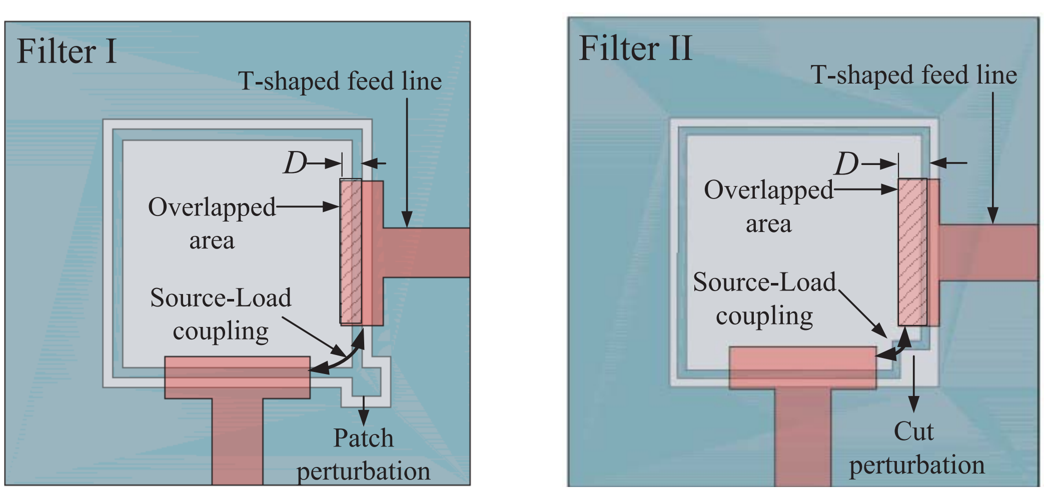

Figure 6. Configuration of two types of dual-mode CPW SLR filters with source-load coupling.

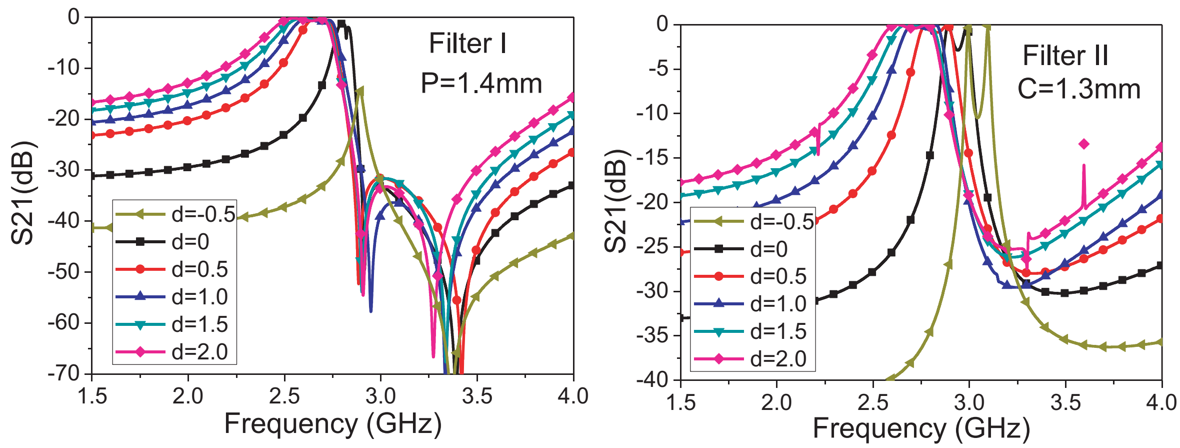

Figure 7. Transmission response of two types of dual-mode CPW SLR filters.

conveniently, and a transmission zero shifts from the low side to the high side of the passband for filter I, while an additional transmission zero emerges on high side of filter II. At the same time, the resonant frequency also decreases when the feed lines have more overlapped area with the resonator. With the overlapped length D increased, a stronger external coupling coefficient as well as a good bandpass filtering response is achieved, as shown in Fig. 7.

5. DUAL MODE FILTER DESIGN AND MEASUREMENT

In order to verify the theory, we design a CPW SLR filter with a patch as an example. The configuration and equivalent circuit of the filter are illustrated in Fig. 8, where resonant loops 1 and 2 represent the two degenerate modes (even mode and odd mode) due to a mode split by the patch perturbation, and the resonant frequency of each loop is affected by the internal coupling strength varying with the physical geometry of the patch. In addition, the source and load of the filter not only provide external coupling to the two resonant modes through the feed lines, such as J_{0i}, $J_{i3}\,(i = 1, 2)$, but also have a source-load coupling J_{03}.

The dimension of the proposed filter is 22.4 mm × 22.4 mm, and the main parameter values are finally designed as $L_1 = 13\,\text{mm}$, $L_2 = 7.2\,\text{mm}$, $G = 0.5\,\text{mm}$, $W_2 = 0.5\,\text{mm}$, $W_3 = 2.2\,\text{mm}$, $W_0 = 2.8\,\text{mm}$, $D = 2.7\,\text{mm}$, $P = 1.3\,\text{mm}$. Such a dual-mode filter is fabricated on a substrate with a permittivity of 9.6 and a thickness of 0.8 mm. Fig. 9 shows photographs of the fabricated filter. The simulated

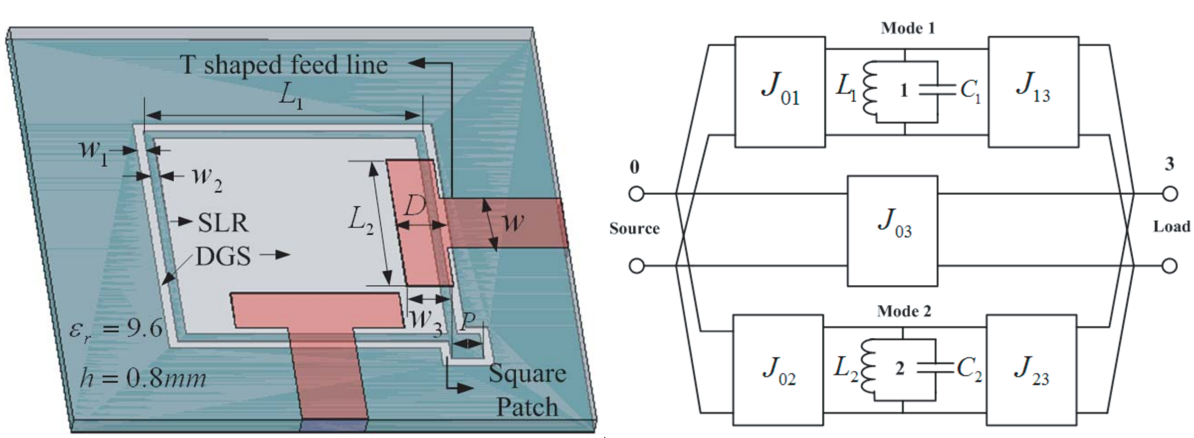

Figure 8. Configuration and equivalent circuit of the dual-mode CPW SLR filter with a patch.

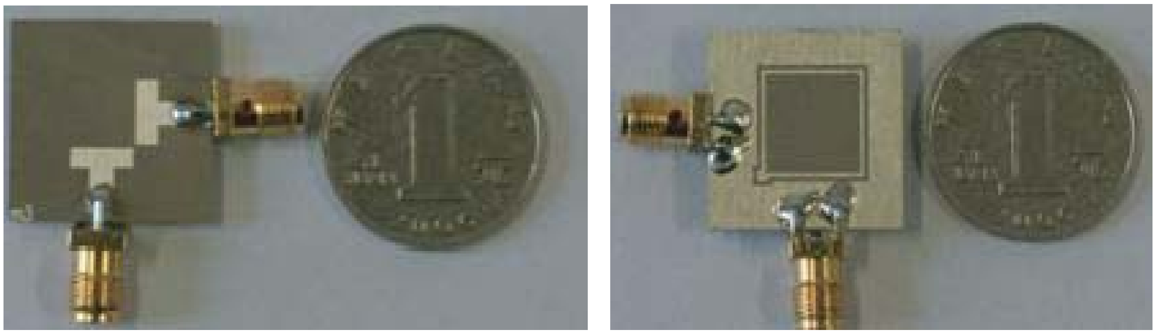

(a) (b)

Figure 9. Photographs of the fabricated dual-mode filter. (a) Top view. (b) Bottom view.

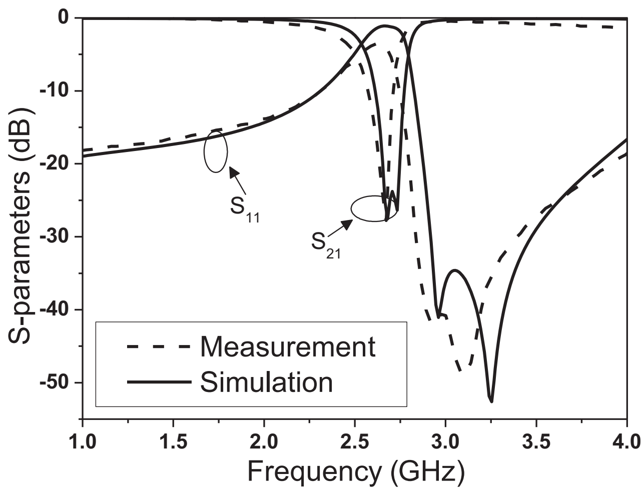

Figure 10. Comparison of the simulated and measured results.

and measured results are compared as shown in Fig. 10. The simulated center frequency is 2.68 GHz, where the insertion loss is about 1.2 dB. As a result of source-load coupling, two transmission zeros appear at 2.96 GHz and 3.25 GHz, which can greatly improve the high-side selectivity of bandpass filter. The measured center frequency has a little shift towards the lower frequency due to the inaccuracy in fabrication and implementation. In addition, the insertion loss at center frequency is about 2.5 dB larger than that in the simulation, which is mainly due to the conductor loss and radiation loss of the resonator DGS. The loss can be reduced by placing the filter in a metal shield with dielectric support.

6. CONCLUSION

In this paper, a novel dual-mode bandpass filter using CPW SLR is presented. The resonant property of CPW SLR is analyzed in theory and investigated by full-wave simulation. A patch or a cut at the corner of the SLR introduces a perturbation and leads to the split of degenerate modes. The additional source-load coupling produces two transmission zeros on the high frequency sideband. Finally, an asymmetric dual-mode filter is designed and fabricated. Numerical simulation using Ansoft HFSS software shows a good agreement with the experiment. It has been shown that the proposed dual-mode filter can provide good selection and convenience of tuning the transmission zeros.

REFERENCES

1. Wolff, I., "Microstrip bandpass filter using degenerate modes of a microstrip ring resonator," *Electronics Letters*, Vol. 8, No. 12, 302–303, 1972.
2. Li, Y. J., Y. Liu, L. Y. Feng, X. Y. Liu, and D. Cheng, "Design of multi-band bandpass filters using short-circuited stub meander loop resonator," *2018 International Conference on Microwave and Millimeter Wave Technology (ICMMT)*, 2018.
3. Görür, A., "Description of coupling between degenerate modes of a dual-mode microstrip loop resonator using a novel perturbation arrangement and its dual-mode bandpass filter applications," *IEEE Transactions on Microwave Theory and Techniques*, Vol. 52, No. 2, 671–677, 2004.
4. Ieu, W., D. Zhou, D. Zhang, and D. Lv, "Compact dual-mode dual-band HMSIW bandpass filters using source-load coupling with multiple transmission zeros," *Electronics Letters*, Vol. 55, No. 4, 210–212, 2019.
5. Liu, H., B. Ren, S. Hu, X. Guan, and P. Wen, "High-order dual-band superconducting bandpass filter with controllable bandwidths and multitransmission zeros," *IEEE Transactions on Microwave Theory and Techniques*, Vol. 65, No. 10, 3813–3823, 2017.
6. Cassinese, A., M. Barra, and W. Ciccognani, "Miniaturized superconducting filter realized by using dual-mode and stepped resonators," *IEEE Transactions on Microwave Theory and Techniques*, Vol. 52, No. 1, 650–654, 2004.
7. Deng, J.-Y., M.-J. Li, D. Sun, L.-X. Guo, and X.-H. Ma, "Compact dual-band inverted-microstrip ridge gap waveguide bandpass filter," *IEEE Transactions on Microwave Theory and Techniques*, Vol. 52, No. 1, 650–654, 2020.
8. Altaf, A., C. Xi, W. Shahzad, U. Dilshad, and J. Miao, "Design of millimeter-wave microstrip BPF using dual-mode ring resonator and folded half-wavelength resonators," *2020 17th IBCAST*, 2020.
9. Iqbal, A., J. J. Tiang, and C. K. Lee, "Dual-band half mode substrate integrated waveguide filter with independently tunable bands," *IEEE Transactions on Circuits and Systems*, Vol. 67, No. 2, 285–289, 2020.
10. Ma, P., B. Wei, J. Hong, B. Cao, X. Guo, and L. Jiang, "Design of dual-mode dual-band superconducting filters," *IEEE Transactions on Applied Superconductivity*, Vol. 27, No. 17, 1724–1732, 2017.
11. Cheng, Y., C. Mei, and L. Zhu, "Design of dual-mode band-pass filter with novel perturbation elements," *Progress In Electromagnetics Research C*, Vol. 96, 59–71, 2019.
12. Nosrati, A., M. Mohammad-Taheri, and M. Nosrati, "Gap-coupled dual-band evanescent-mode substrate integrated band-pass filter waveguide," *Progress In Electromagnetics Research Letters*, Vol. 89, 53–59, 2020.